This article has been accepted for publication in a future issue of this journal, but has not been fully edited. Content may change prior to final publication. Citation information: DOI 10.1109/JIOT.2019.2906838, IEEE Internet of Things Journal

LoRaWAN Network: Radio Propagation Models and Performance Evaluation in Various Environments in Lebanon

Rida El Chall, Samer Lahoud, and Melhem El Helou, *Senior Member, IEEE*

***Abstract*—Recently, LoRaWAN has emerged as a promising technology for the Internet of things (IoT), owing its ability to support low-power and long-range communications. However, real-world deployment and network optimization require accurate path-loss (PL) modeling, so as to estimate network coverage, performance, and profitability. For that reason, in this work, LoRaWAN radio channel is investigated in the 868 MHz band. Extensive measurement campaigns were carried out in both indoor and outdoor environments at urban and rural locations in Lebanon (Saint Joseph University of Beirut campus, Beirut city, and Bekaa valley). Based on empirical results, PL models are developed for LoRaWAN communications and compared with widely used empirical models. Moreover, the performance and the coverage of LoRaWAN deployment are evaluated based on real measurements. The results show that the proposed PL models are accurate and simple to be applied in Lebanon and other similar locations. Coverage ranges up to 8 km and 45 km were obtained in urban and rural areas, respectively. This reveals the reliability of this promising technology for long-range IoT communications.**

***Index Terms*—LPWAN, IoT, LoRa, LoRaWAN, long range, path-loss model, outdoor, indoor, urban, rural**

I. Introduction

THE Internet of things (IoT) is a promising paradigm that is rapidly evolving to make any device part of the internet environment. According to Cisco, it is expected that more than 50 billion devices will be connected through radio communications by 2020 [1]. IoT devices will be used in wide range of applications including security, industrial monitoring, smart homes, smart cities, smart agriculture, etc. Comprehensive surveys on the emerging IoT technologies and their challenges have been reported in [2], [3].

The main characteristics and requirements of IoT applications are long range, low data rate, low energy consumption, and cost-effectiveness. Low-power wide area networks (LPWAN) have been therefore developed to meet these diverse requirements. LPWANs typically operate in licensed and unlicensed frequency bands. Many LPWAN technologies have been investigated by different standards and industrial consortia, including LoRa, Sigfox, NB-IoT, ECGSM-IoT, Random Phase Multiple Access (RPMA), Weightless, DASH7 alliance, etc. An overview and comparison of these emerging LPWAN technologies have been presented in [4]–[7]. In particular, LoRaWAN is one of the most deployed LPWAN technology, gaining greater interest from the research and industrial communities. From theoretical aspects, many studies have focused on the performance and characteristics of LoRaWAN communications. An overview of the capabilities and the limitations of LoRaWAN has been presented in [8]. Theoretical evaluation of the capacity and scalability has also been performed [9], [10]. Moreover, an adaptive configuration of LoRa networks has been proposed for scalable IoT deployments [11]. The impact of physical settings such as spreading factor, coding rate and bandwidth on the data rate and time on air have been investigated [12]. All these works concluded that LoRaWAN systems should be carefully configured and dimensioned to achieve a good tradeoff between scalability and efficiency.

On the other hand, physical and link layer performance of LoRa/LoRaWAN have been evaluated experimentally by field tests [13]–[15]. The experimental tests have been conducted in various real-world environments ranging from indoor [16]–[18] and urban/suburban [19]–[23] to maritime [20], rural [23] and mountain [24] scenarios. The experiments show communication ranges from 10 to 30 km in rural areas and 2 to 8 km in urban areas. Furthermore, the impact of environmental factors such as temperature and vegetation has been investigated [24], [25]. It has been shown that vegetation and higher temperature significantly reduce communication ranges. In case of indoor operation, results showed that LoRa can achieve good coverage in the entire buildings of Oulu campus University [17]. However, connectivity issues and high packet losses might be encountered in the basement [16], whereas the best coverage is achieved when the receiver is located on the roof rather than in the basement [18]. Different kinds of applications have been tested using LoRa, such as vehicle to grid communications [26], health monitoring [27], [28], and river monitoring [29].

The key parameters to optimize network performance prior to real deployment is to correctly predict the coverage and to carefully adjust antenna heights of installation sites. Therefore, precise modeling of radio propagation characteristics is very crucial for LoRaWAN network planning and optimization. Radio propagation characteristics have been widely studied over the world. Numerous field measurements have been carried out in various indoor and outdoor environments in the context of cellular and wireless sensor networks. Generally, the path-loss (PL) is impacted by many factors such as distance, frequency band, average antenna heights, geography and terrain in terms of obstacles, buildings, hills, mountains, people, etc. However for the indoor environment, additional factors need to be considered such as floor plans, walls, and type and thickness of building materials. Several PL models applicable to outdoor environments for the [800 - 1800] MHz and [2.5-5] GHz bands are developed by research institutes and standard organizations, *e.g.*, Okumura-Hata, Cost 231-Hata,

The authors are with the Ecole Supérieure d'Ingénieurs de Beyrouth (ESIB), Faculty of Engineering, Saint Joseph University of Beirut, Beirut 1107 2050, Lebanon (e-mail: rida.chall@gmail.com; samer.lahoud@usj.edu.lb; melhem.helou@usj.edu.lb).

Manuscript received December 2, 2018; revised Feb 21, 2019.

This article has been accepted for publication in a future issue of this journal, but has not been fully edited. Content may change prior to final publication. Citation information: DOI 10.1109/JIOT.2019.2906838, IEEE Internet of Things Journal

Bertoni-Walfisch, ITU Advanced, WINNER II, WINNER+, and 3GPP Spatial Channel Model [30]–[35]. Similarly, many indoor propagation models are proposed in literature, *e.g.* ITU-R P1238, IEEE 802.11n, 3GPP, Cost 231 multi-wall, and Motley-Keenan [31], [35]–[38]. Although many of these PL models are widely used today, they are not intended for long-range LoRaWAN network operating at 868 MHz band. For this reason, a channel attenuation model has been derived from the data measurements in the city of Oulu, Finland [20]. In [39], an urban PL model is proposed for LoRa links in Dortmund, Germany. An empirical evaluation of the indoor propagation performance of LoRa at Glasgow Caledonian university has been presented, showing that the multi-wall model has the best overall performance [40]. However, other factors have to be considered such as end-device antenna heights and harsh environmental conditions due to the variety of IoT applications. Moreover, irregular terrain profile and topography variation have to be considered, *e.g.* hilly Mediterranean and mountain topography in Lebanon. Consequently, more field measurements are required to accurately elaborate and validate radio propagation models for optimal deployment of LoRaWAN in both indoor and outdoor environments.

Focusing on those important issues, this paper presents an in-depth study of the radio propagation characteristics, considering different environments and antenna heights in the 868 MHz band in Lebanon. Extensive measurement campaigns were carried out in both indoor and outdoor environment at rural and urban areas. The set of measurement data is publicly available in [41]. In particular, indoor and outdoor tests were performed in the Saint Joseph University (USJ) of Beirut campus. Urban and rural tests were conducted in Beirut city and Bekaa valley, respectively. Based on empirical results, we derive PL models for Lora communications at the 868 MHz band under various parameters. The proposed models are compared with some widely used empirical indoor/outdoor PL models, to determine their accuracy. We show that the proposed PL models fit measurements with more accuracy and simplicity compared to other models. Moreover, the performance and coverage of LoRaWAN deployment is evaluated. The results show coverage ranges up to 8 km and 45 Km in urban and rural areas, respectively.

The remainder of this paper is organized in the following way. Section 2 provides an overview of LoRa and LoRaWAN technology. Section 3 presents channel modeling principles for both indoor and outdoor environments and reviews the most widely used PL models. Section 4 describes measurement campaigns carried out in Lebanon at different environments. In section 5, the results are analyzed and discussed. The PL models are therefore developed and compared with others. Finally, the conclusions are drawn in Section 6.

II. LoRa and LoRaWAN Overview

This section provides an overview of LoRaWAN technology. First, LoRa physical layer is presented followed by a description of LoRaWAN link protocol and basic network architecture.

A. LoRa PHY Layer

LoRa is a physical layer technology developed and commercialized by Semtech for long-range and low-power communications [42]. It is a derivative of chirp spread spectrum (CSS) modulation with integrated forward error correction (FEC) [43]. CSS technique allows to increase the receiver sensitivity, enabling long communications ranges. It actually allows to correctly decode transmissions 19.5 dB below the noise floor (maximum link budget of 150 dB) [43].

Generally, LoRa is characterized by five configured parameters: carrier frequency (CF), bandwidth (BW), transmission power (P_{tx}), spreading factor (SF), and coding rate (CR). These parameters can be tuned for a tradeoff among several features: data rate, transmission range, robustness to interference, and energy consumption. LoRa operates on the sub-1GHz bands, *e.g.* 433, 868 or 915 MHz ISM bands, depending on the region in which it is deployed. In Europe, 433 MHz and 868 MHz are available, with 868 MHz being most commonly used. The bandwidth can be 125 kHz, 250 kHz, and 500 kHz. A higher bandwidth corresponds to a higher data rate, but to a lower sensitivity. The transmit power can be configured based on the region and the band used for transmissions. The SF represents the ratio between symbol rate and chip rate. The supported SF values range from 7 to 12. A higher SF makes the signal more robust to noise (increase the sensitivity and range) but decreases the data rate. Note that each of the available SFs are orthogonal, enabling multiple signals to be transmitted on the same channel simultaneously [43]. LoRa uses also FEC to perform error detection and correction. Coding rate can be set to $4/(CR+4)$ with $CR \in \{1, 2, 3, 4\}$. Depending on the configuration of the physical layer parameters, the bit rate ranges from 0.3 kbps to 50 kbps as shown in Table I. It is worth noting that different LoRa configurations are referred to as data rates (DR) in LoRaWAN specification.

TABLE I: Data rate and sensitivity of different LoRa configuration parameters for the 868 MHz band.

Data rate	Spreading factor	Bandwidth [KHz]	Bit rate [kbps]	Sensitivity [dBm]
DR 0	12	125	0.293	-137
DR 1	11	125	0.537	-134.5
DR 2	10	125	0.976	-132
DR 3	9	125	1.757	-129
DR 4	8	125	3.125	-126
DR 5	7	125	5.4680	-123
DR 6	7	250	10.936	-122

B. LoRaWAN Link Layer

LoRaWAN is the upper layer protocol for LoRa, described in an open specification and developed by the LoRa Alliance [44]. LoRaWAN relies on an ALOHA-based MAC protocol to reduce the complexity of end-devices in accessing the channel. The network architecture is a star-of-stars topology and consists of three entities: end-devices (EDs), gateways (GWs), and a network server as illustrated in Figure 1. EDs communicate with GWs using single-hop LoRa communication. The GW simply relays received messages to a central network server via an IP backbone. The central network server manages the network access and provides mobility, frame control as well as security functions.

This article has been accepted for publication in a future issue of this journal, but has not been fully edited. Content may change prior to final publication. Citation information: DOI 10.1109/JIOT.2019.2906838, IEEE Internet of Things Journal

LoRaWAN introduces three classes: Class A (the default), Class B and Class C (both optional). Class A supports basic bi-directional communications, where each uplink transmission is followed by two short receive windows for transferring data to the ED. Class B extends Class A by adding extra receive windows at scheduled times. The GW then periodically broadcasts beacons to maintain the synchronization of EDs, while EDs of Class C have almost continuously receive windows when not transmitting.

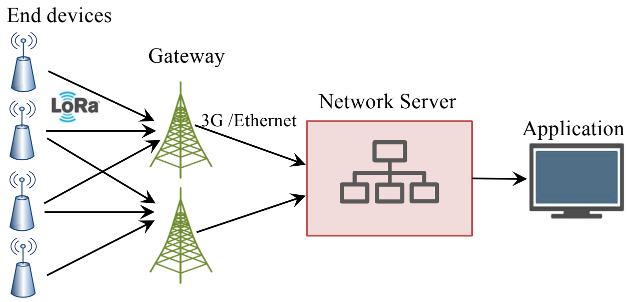

Fig. 1: LoRaWAN architecture.

Three default channels (868.1, 868.3 and 868.5 MHz) must be implemented in every LoRaWAN network. In practice, a physical channel is chosen on a pseudo-random basis, based on regularity requirements defined by ETSI [45]. Each sub-band has specific requirements regarding maximum effective radiated power (ERP), and duty cycle limits. For the majority of sub-bands, the ERP is 25 mW (14 dBm) and the duty cycle limits vary between 0.1% and 1%. Furthermore, LoRaWAN specification defines an adaptive data rate (ADR) scheme which enables the server to set the spreading factor of each node, maximizing the battery lifetime while optimizing the overall network capacity. The maximum MAC payload can range from 59 to 250 bytes depending on LoRa configurations. LoRaWAN overhead per packet is 13 bytes.

III. Radio Propagation Models

Radio waves take several ways when traveling between transmitter and receiver, resulting in a significant loss in the received signal. This loss may be due to many effects including reflection, diffraction, refraction, and scattering components resulting from buildings, trees, hills and other obstacles.

Channel measurements aim to understand the channel behavior and to develop realistic and trustworthy channel models. Generally, propagation models include deterministic models and empirical models. Deterministic models are very complex since they require detailed knowledge of location, dimension and physical parameters of every obstacles in the area. However in empirical models, the parameter values are derived by fitting measurement data to an appropriate function for a particular environment. This gives more generic model that can be used by systems operating in similar areas. Herein empirical propagation models used in this paper are presented. These models will be adapted according to our measurements in Lebanon, as discussed in Section V.

A. Free-Space PL Model

Free-space model is a baseline model that provides a measure of path-loss when the transmitter and receiver are within line-of-sight (LOS) range without any obstacles between them. It is based on the Friis' free-space transmission equation, given in the logarithmic domain as follows:

$$PL_{FS}(d)[dB] = 20\log_{10}(f) + 20\log_{10}(d) + 32.44, \quad (1)$$

where d is the distance between the transmitter and the receiver in km, and f is the frequency in MHz.

B. Log-distance PL Model

The log-distance propagation model, also referred as one-slop model, is a general PL model that has been used in a large number of indoor and outdoor environments. It assumes that PL varies exponentially with distance according to the following equation:

$$PL(d)[dB] = 10n\log_{10}(d/d_0) + PL_0 + X_\sigma, \quad (2)$$

where n is the PL exponent, d is the distance between the transmitter and the receiver, and PL_0 is the PL at a reference distance d_0. Shadow fading is represented by a zero-mean Gaussian random variable X_σ with standard deviation σ (in dB). The PL parameters are derived from a regression or fitting curve over the measured data and depend upon the environment. For instance, $n = 2.32$ and $PL_0 = 128.95$ in the city of Oulu (Finland) [20], whereas $n = 2.65$ and $PL_0 = 132.25$ in the city of Dortmund (Germany) [39].

C. Multi-Wall-and-Floor (MWF) Model

In order to characterize the PL within buildings, the most accurate approach is to consider additional attenuation incurred by walls and floors. Thus, PL is modeled as:

$$PL(d)[dB] = 10n\log_{10}(d/d_0) + PL_0 + WAF + FAF, \quad (3)$$

where WAF and FAF are wall and floor attenuation factors based on the number of traversed walls n_w and floors n_f between the transmitter and the receiver, respectively. These factors can be extracted by ray tracing techniques or empirical measurements. Actually, the penetration losses of walls and floors depend on several factors such as frequency, thickness and material of obstacles. Measurement results show either a linear or a nonlinear relation between the traversed walls or floors and the penetration loss. Examples of MWF models are Cost 231-MWF and Motley-Kennan. In both models, WAF is proportional to the number of penetrated walls, $WAF = \sum n_{wi}L_{wi}$, where n_{wi} is the number of walls of type i and L_{wi} is the penetration loss for the wall of type i. In Motley-Kennan model, FAF is expressed by a floor loss factor L_f multiplied by the number of floors ($FAF = n_f L_f$). Cost 231-MWF model provides a nonlinear function of floor attenuation which increases more slowly as per additional floors: $FAF = L_f n_f^{((n_f+2)/(n_f+1)-b)}$, where b is an empirical constant selected to obtain a suitable fit of the measured data. A similar approach is taken by ITU-R model [36], where only the floor loss is considered.

D. Summary of PL Models

Looking into the literature, a lot of field measurements were carried out to model the PL in different environments and frequency bands. The characteristics of the most used PL models are shown in Table II. Their applicability ranges and their environments are specified. Okumura-Hata model is an empirical method, based upon extensive measurements made in Tokyo city between 200 MHz and 2 GHz [30].

This model specifies four generic categories of environments: large cities, medium-small cities, suburban areas, and rural areas. It assumes that there are no dominant obstacles between the base station and the mobile, and that the terrain profile changes slowly. Cost 231-Hata model extends Okumura-Hata model for medium to small cities to cover the band [1500-2000] MHz [31]. The International Telecommunications Union (ITU) has also defined a set of channel models for the evaluation of advanced mobile system proposals [32]. The ITU advanced models apply the same approach as 3GPP/3GPP2 models. These models are primarily based on extensive measurement campaigns mostly done within the framework of the European projects WINNER I and WINNER II [33]. Scenarios specified in 3GPP include indoor hotspot (InH), urban microcell (UMi), urban/suburban macrocell (UMa/SMa) and rural macrocell (RMa) [35]. The 3GPP developed models can be applied in the frequency range of 2 to 6 GHz (0.46 to 6 GHz for RMa) for different antenna heights. These models consider further parameters such as the average building height h and the street width W. For indoor environment, ITU-R model and Cost-231 MWF were considered.

It should be mentioned that these models have been proposed in the context of cellular and wireless sensor networks. Their applicability ranges show some limitations in terms of antenna heights and terrain profiles. For instance, the base station antenna height has a maximum of 200 m, while the user has a minimum antenna height of 1 m, assuming a flat terrain. This motivates additional studies for PL modeling to investigate the validity of these models for long-range LoRAWAN deployment, considering low antenna heights for the user, and irregular terrain profile as presented in the following sections.

IV. Measurement Campaigns

This section describes measurement campaigns carried out in Lebanon in order to study the PL characteristics of the 868 MHz band under different ED antenna heights and environment conditions. The experimental platform is first described followed by a presentation of the different sites.

A. Measurement Setup

The experimental platform used in our measurement campaigns is depicted in Figure 2. Pycom LoPy with PyTrack expansion board was used as LoRa ED [46], powered by 3.7-volt rechargeable lithium battery. The LoPy has an integrated LoRa SX1272 transceiver and an additional WiFi transceiver. PyTrack module includes an embedded global positioning system (GPS) used to obtain the location of the ED. Kerlink Wirnet Station was used as the GW which is able to receive LoRa frames from -20 dBm to -141 dBm, depending on the LoRa BW and SF [47]. The GW was connected to the network server provided by an open source LoRa server (https://www.loraserver.io.). Both GW and ED use an omnidirectional dipole antenna of 3 dBi gain. Upon the reception of each frame, the GW provided the received signal strength indicator ($RSSI$), the signal-to-noise ratio (SNR), and the payload message. These received parameters were recorded on the server side for further analysis and processing. The quality of reception can be monitored in real-time with an MQTT web client application.

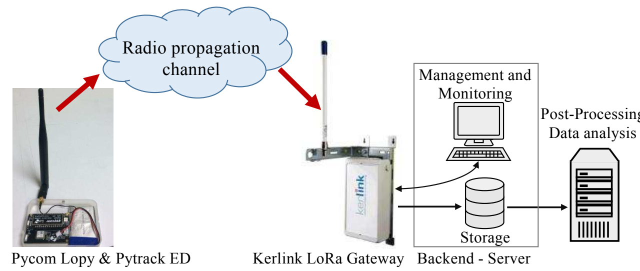

Fig. 2: Platform used in the measurement campaigns.

The ED was configured to send a packet every 10 seconds, with GPS coordinates included in the payload field. The packets also include a sequential number, in order to identify the packet loss. No mechanisms for control and automatic retransmissions were used. The transmit power was set to 14 dBm, SF to 12 (to achieve the best receiver sensitivity), and the BW to 125 kHz, using the 3 default channels (868.1, 868.3 and 868.5 MHz). The packet payload was 50 and 37 bytes including 13 bytes MAC header in case of indoor and outdoor setups, respectively. The measurement setup parameters are listed in Table III. During all the measurements the position of GWs was fixed, whereas the ED was moved to different locations. For urban and indoor scenarios, the GW was installed at the rooftop of the ESIB-USJ engineering building at a height of 12 m above ground level, being at a final altitude of 260 m above sea-level. For the rural area, the GW was placed on the rooftop of Kefraya tower at a height of 12 m above ground level, being at a final altitude of 970 m above sea-level (Figure 3). For outdoor usage, various antenna heights were considered for the ED to reflect different envisioned IoT applications. The ED was mounted on a tripod at 3 heights: near-ground at 20 cm, 1.5 m and 3 m as shown in Figure 3. However in the indoor environment, there is no interest to consider different ED antenna heights due to the penetration losses through walls and floors. Moreover, drive tests were performed in urban and rural areas, where ED was attached to the roof-rack of a car approximately at 1.7 m height of the ground (Figure 3). During the drive test, the vehicle speed was around 30 to 40 km/h.

In order to calculate the PL, the received signal strength P_{rx} is estimated based on both the SNR and the $RSSI$ [47]. If $SNR > 0$, $P_{rx} = RSSI$, otherwise, $P_{rx} = RSSI + SNR$. The PL is therefore computed as follows:

$$PL = P_{tx} - P_{rx} + G_{tx} + G_{rx} - L_{tx} - L_{rx}, \quad (4)$$

where P_{tx} is the transmit power in dBm. G_{tx} and G_{rx} are

TABLE II: Summary of PL models.

PL Model	Environment	Applicability Ranges
Free-space	All (basic model)	LOS
Okumura-Hata [30]	Urban (large & small cities) Suburban Rural	f = [150-1500] MHz $h_b = [30 - 200]$ m, $h_m = 1 - 10$ m d = [1-20] km
Cost 231-Hata [31]	Urban large & small cities	f = [500-2000] MHz $h_b = [30 - 200]$ m, $h_m = [1 - 10]$ m d = [1-20] km
WINNER II Table 4.4 in [33]	A-D scenarios, *e.g.* indoor office, indoor-to-outdoor, urban microcell /macrocell, rural macrocell	f = [2-6] GHz
WINNER+ Table 4-1 in [34]	Similar to WINNER II Extended to 800 MHz band	f = [0.45-6] GHz
3GPP TR 36.814 based on WINNER II Table B1.2.1-1 in [35]	Indoor hotspot (InH), Urban microcell (UMi) Urban/Suburban macrocell (UMa, SMa) Rural macrocell RMa	f = [2-6] GHz, [0.46-6] GHz (RMa) h_{BS} = [10-150] m, h_{UE} = [1-10] m h = [5-50] m, W = [5-50] m
ITU-R P.1238 [36]	Indoor (residential, office, commercial) *e.g.* office at 900 MHz: N = 33, L_f(1,2,3) = 9,19,24	f =900 MHz to 5.2 GHz $n_f = [1 - 4]$, d¿1 m
Cost-231 MWF [31]	Indoor (buildings) wall and floor losses	f =900, 1800 MHz *e.g.* L_f = 14.8 dB, L_w =1.9 dB

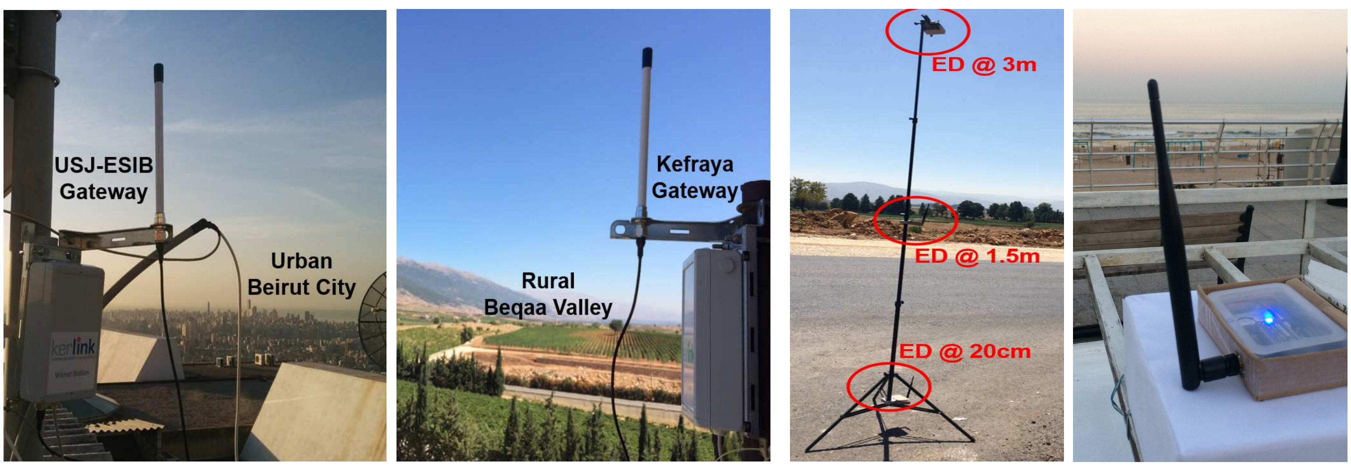

(a) (b) (c) (d)

Fig. 3: Locations of Lora gateways and end-devices: (a) ESIB-USJ GW, (b) Kefraya GW, (c) Pycom Lopy EDs mounted on a tripod at 3 heights, (d) ED mounted on the roof-rack of a car.

TABLE III: Measurement setup parameters

Parameter	Value
End-Device (ED)	Pycom Lopy with Pytrack (SX1272)
Gateway (GW)	Kerlink (SX1257, SX1301)
Tx Power	14 dBm
Frequency	868.1, 868.3, and 868.5 MHz
Bandwidth (BW)	125 kHz
ED/GW antenna	3 dBi omnidirectional
Spreading factor (SF)	12
Coding rate	4/5
Payload Length	50 bytes (outdoor), 37 bytes (indoor)
Time interval	10 sec
Traffic	Uplink , No-ACK
ED antenna height	20 cm, 1.5 m, 3 m (Outdoor)
GW effective antenna height	200 m (ESIB-USJ), 70 m (Kefraya)

the transmitter and the receiver antenna gains, respectively. L_{tx} and L_{rx} represent the transmitter and receiver losses due to cables, assumed negligible in this work. The shadowing is classically characterized by a zero-mean Gaussian variable with standard deviation σ. This standard deviation describes the dispersion between measured and expected PLs.

Furthermore, the performance of LoRaWAN was evaluated during experiments using additional metrics. The SNR indicates the quality of the received signal. The packet delivery ratio (PDR) which is the ratio between received and transmitted packets, indicates the reliability of communications. The coverage range is the measured distance between GW and ED, when the PDR was above a certain threshold (*e.g.* 90%).

B. Experimental Environments

Our experiments were performed in three locations in Lebanon, with different environmental characteristics as summarized in Table IV.

TABLE IV: Characteristics of the experimental sites.

Environment	Location / Characteristics	GW/ED deployment
Indoor	USJ multi-floor building offices, classes, corridor, floors, walls	ESIB-USJ GW h_{GW} = 12 m ED in different floors
Outdoor *Suburban*	USJ Campus (high shadowing area) Medium density of users, buildings up to 4 floors, trees, mountains	ESIB-USJ GW $h_{GW} = 12$ m $h_{ED} = [0.2 - 3]$ m
Urban	Beirut City High density of users, buildings more than 4 floors	ESIB-USJ GW, effective height = 200 m $h_{ED} = [0.2 - 3]$ m
Rural	Bekaa Valley Low density of users, vegetation, trees, hills	Kefraya GW, effective height = 70 m $h_{ED} = [0.2 - 3]$ m

Indoor and outdoor tests were conducted in the campus of ESIB-USJ. The urban area is located in the city of Beirut, whereas rural area is situated in Bekaa valley. Indoor measurements were performed in multi-floor buildings connected together by indoor passages on the ESIB-USJ campus as shown in Figure 4. These buildings, mostly built of concrete and steel, differ in geometry and usage, with dimensions of $110\,\text{m}\times 50\,\text{m}$. Different conditions and constraints (indoor and deep-indoor) were considered such as offices, classes with obstacles, corridor, etc. We considered 70 locations of ED with distance of 5 m to 110 m on 4 different floors ranging from the basement to the 4^{th} floor. At each location, 20 measurements were taken. We have used the available floor plan while conducting our measures to mark the positions of ED as illustrated in Figure 4. This helps us to compute the distance and to count the number of floors and walls or obstacles between the transmitter and the receiver. A total amount of 1400 measurements was collected.

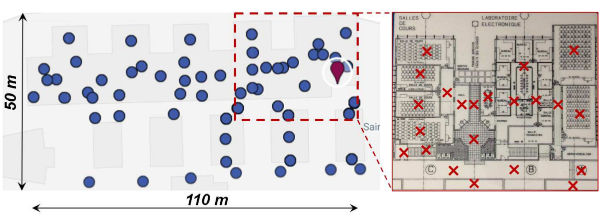

Fig. 4: Map of the indoor environment at USJ campus showing the measurement locations of EDs.

The outdoor test in USJ campus was realized by moving the ED, emitting continuously around the campus as shown in Figure 5. The campus area is about 200 m north to south and 280 m east to west. It is a mixed environment composed of a combination of medium building heights, green spaces with trees, having medium population density. The distance between ED and GW varied in the range of 5 m to 200 m. In this experiment, 2200 different measurements were recorded.
The urban measurements were conducted in the city of Beirut in Lebanon, which is a densely populated city (over 360 000) characterized by a high density of buildings, gardens, roads, and commercial/industrial facilities. The measurements were performed within an area of $60\,\text{km}^2$ having diverse topography with some terrain elevation changes. The effective terrain height is about 60 m. We considered 35 fixed point measurements around the GW with a distance up to 9 km as illustrated in Figure 6. These locations were selected to study the influence of location and environment on the performance of LoRaWAN, *e.g.* park areas, commercial centers, main roads, airport areas, port areas. On each of these measured points, the aforementioned antenna heights were considered for the ED, where 25 packets were sent for each realization. A total amount of 2600 measurements was collected.

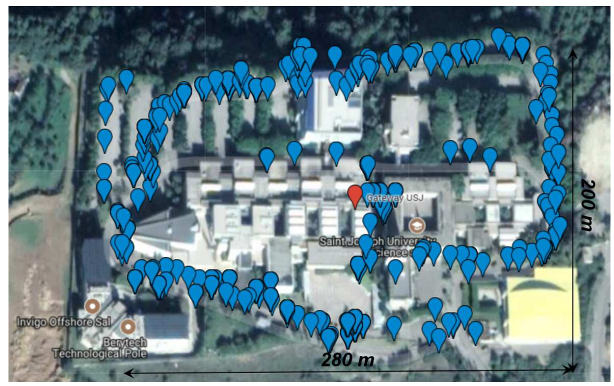

Fig. 5: Map of the outdoor environment at USJ campus showing the measurement locations of EDs.

The rural environment is Bekaa valley on Joub Jannine-Bar Elias road, located at an altitude of 900 m above sea-level. This area is almost flat with small hills of 20 to 30 m height difference, being surrounded by open fields, farmland and small hills with a lack of buildings and other obstacles. Measurements were made at 30 locations in LOS and NLOS conditions up to 20 km from the GW located at Kefraya tower as shown in Figure 3. Similarly to urban experiments, 3 antenna heights were used for EDs. A total amount of 2200 measurements was collected.

V. Results and Discussion

In this section, we present the results of measurements conducted in Lebanon as described in Section IV. First, we derive PL models for the different environments (indoor, outdoor, urban, and rural). Next, the proposed PL models are compared with widely used empirical models. The performance and the coverage of LoRaWAN are also evaluated. Note that the presented results were obtained for the uplink communication.

A. Indoor Results

In the indoor environment, we investigate the impact of wall and floor penetration losses on the received signal. Figure 7 shows the PL values at different ED-GW distances and the cumulative distribution function (CDF) of shadowing.

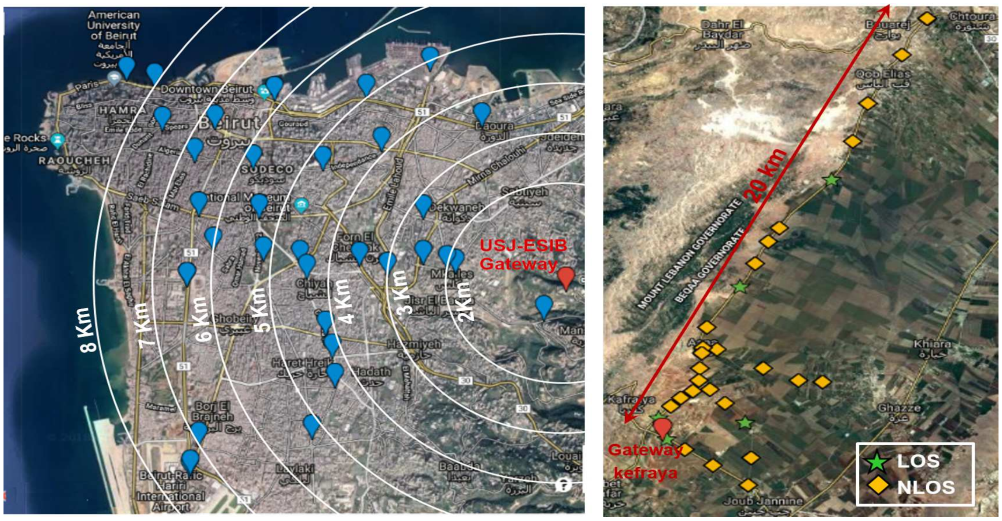

(a) Beirut city (b) Bekaa valley

Fig. 6: Map of urban (a) and rural (b) environments showing measurement locations of EDs.

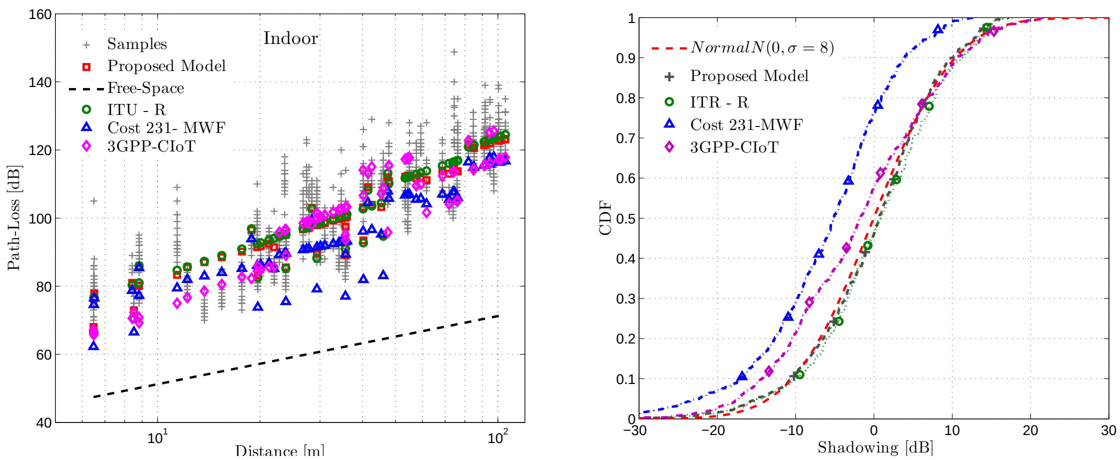

(a) (b)

Fig. 7: Path-loss vs. distance (a) and CDF of shadowing (b) in indoor environment.

It can be noticed that the PL increases almost logarithmically with the distance. We observed, during measurements, that the loss between floors does not increase linearly with the number of floors. The additional loss per floor decreases with the increasing number of floors. For instance, the additional penetration loss was found to be around 8.1, 6.7, 4.3 dB between floor 2, 3 and 4, respectively. This is mainly due to the different propagation mechanisms between floors. In the first floor, the received signal mainly comes through the floors, while the signal in the higher floors may be composed of diffracted paths. Therefore, by using curve fitting techniques and by considering both ITU-R and Cost 231-MWF models, we proposed our PL model as:

$$PL = 10n\log_{10}(d) + PL_0 + n_w L_w + n_f^{\left(\frac{n_f+2}{n_f+1}-b\right)} L_f, \quad (5)$$

where $n = 2.85$ is the indoor PL exponent, $PL_0 = 120.4$ is the reference PL. n_w and n_f are the number of walls and floors, respectively. b was taken equal to 0.47 to obtain a suitable fit. $L_f = 10$ and L_w = 1.41 represent the loss factor of floors and walls, respectively. All floors and walls are assumed identical in this model. The shadowing samples match the Gaussian distribution with a standard deviation of 8 dB. This shadowing is due to the variety of obstacles, *e.g.* desks, offices, etc. It should be mentioned that the obtained PL exponent is close to that used for the office area in ITU-R model (N=33) at 900 MHz. Moreover, we have compared the proposed model with the most used indoor PL models namely ITU-R, Cost 231-MWF, and 3GPP for Cellular-IoT (Figure 7a). The CDF of shadowing samples resulting from the difference between the measured values and estimated values of considered models are also compared in Figure 7b. The proposed model fit measurements with more accuracy compared to other models. Indeed, Free-space model underestimates the measured values as expected. Moreover, the ITU-R model is close to the samples, but it is less accurate than the proposed model due to the lack of additional wall losses. ITU-R model presents a mean and a standard deviation of error of 0.48 and 8.3 dB, respectively. Cost 231-MWF and 3GPP models underestimate the measured values and show a standard deviation of error of 8.7 and 10.2, respectively. This may lead to a high estimation of received signal and consequently to non-covered areas.

This article has been accepted for publication in a future issue of this journal, but has not been fully edited. Content may change prior to final publication. Citation information: DOI 10.1109/JIOT.2019.2906838, IEEE Internet of Things Journal

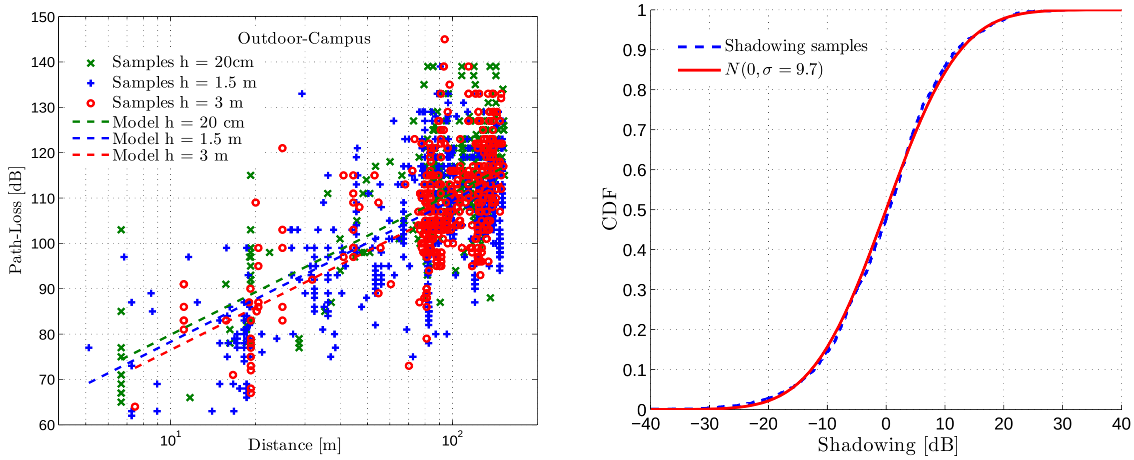

(a) (b)

Fig. 8: Path-loss vs distance (a) and CDF of shadowing (b) in USJ Campus.

Cost 231-MWF considers both floor and wall losses, but it has a PL exponent of 2, leading to the underestimated values. Furthermore, we have considered the locations of EDs in the corridors, and we have obtained a PL exponent of $n = 1.8 - 2$. This range of values is widely considered in the literature for corridor area. The performance of LoRaWAN deployment in terms of PDR and SNR is also evaluated during indoor measurements. Table V summarizes the obtained results in the corridor and in the multi-floor building. The results show an average PDR of 95% and an average SNR of about 9 dB for a distance up to 110 m from the GW. A minimum PDR of 45% was obtained. The minimum SNR and RSSI were observed at a distance of 100 m in the basement. In general, the results indicate a good quality of signal reception and reveal the reliability of using LoRaWAN for effective communications in indoor and deep-indoor deployment.

TABLE V: LoRaWAN Performance in indoor environment.

Location	PDR	SNR [dB]	RSSI [dBm]	min PDR	min SNR	min RSSI
Corridor	0.99	9.48	-61.16	0.9	8.6	-80.2 [28 m]
Building	0.95	8.59	-81.65	0.45	1.92	-110 [100 m]

B. Outdoor Campus Results

In the following, we study the impact of ED antenna height on the received signal and the performance of LoRaWAN in the USJ campus. Figure 8a shows the PL as a function of distance under different ED antenna heights. It can be seen that increasing ED antenna heights improves the received signal strength (reduce PL). Indeed, increasing antenna heights reduces the obstruction of Fresnel zone. In order to derive the expected PL from the measured data, the linear polynomial fit was used as a function of logarithmic distance and ED antenna height as follow:

$$PL = 10n \log_{10}(d) + PL_0 + L_h \log_{10}(h_{ED}) + X_\sigma, \quad (6)$$

where L_h is the additional loss due to the ED antenna height h_{ED}. The fitting process leads to $n = 3.119$, $PL_0 = 140.7$, and $L_h = -4.7$. This means that reducing h_{ED} results in an additional loss of 4.7 dB per decade. The results show a good fit between the proposed model and the measured values. Additionally, the shadowing samples are inline with the Gaussian distribution with zero mean and a standard deviation of 9.7 dB, as shown in Figure 8b. This large value of shadowing is mainly due to the topography variability and the large number of obstacles in this area, as described in Section IV. The campus could be considered as a suburban environment but with high shadowing effect. The performance of LoRaWAN was also evaluated. An average PDR, SNR and RSSI of 80%, 8.5 dB and -86 dB are respectively obtained despite the high shadowing effect in this area.

C. Outdoor Urban Results

In this section, we focus on studying the channel characteristics and the performance of LoRaWAN in an urban environment. Figure 9 shows the effect of ED antenna height on the PL. Similar to the campus results, we can see that by increasing the ED antenna height from 20 cm to 3 m, the PL is reduced by 8 dB. This is explained by the fact that an important part of the Fresnel zone will be obstructed by the ground when lowering antenna height to 20 cm. By contrast, higher antennas would lead to more clear space from obstacles.

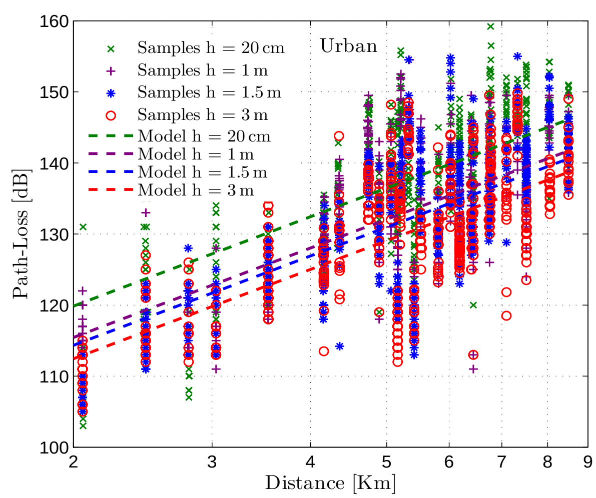

Fig. 9: Path-loss vs distance in urban environment under different ED antenna heights, Beirut city.

This article has been accepted for publication in a future issue of this journal, but has not been fully edited. Content may change prior to final publication. Citation information: DOI 10.1109/JIOT.2019.2906838, IEEE Internet of Things Journal

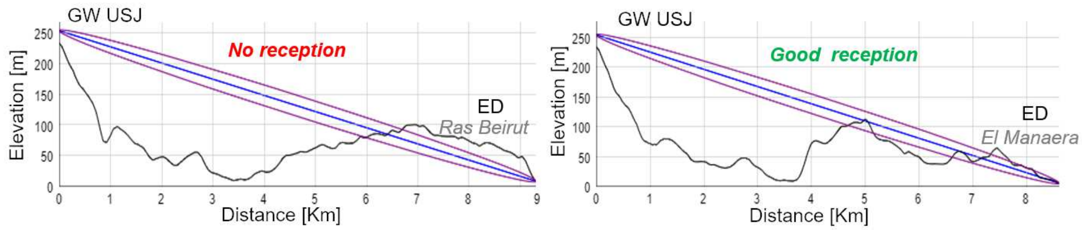

Fig. 10: Example of elevation profile between USJ GW and ED in *Ras Beirut* and *El Manara* locations.

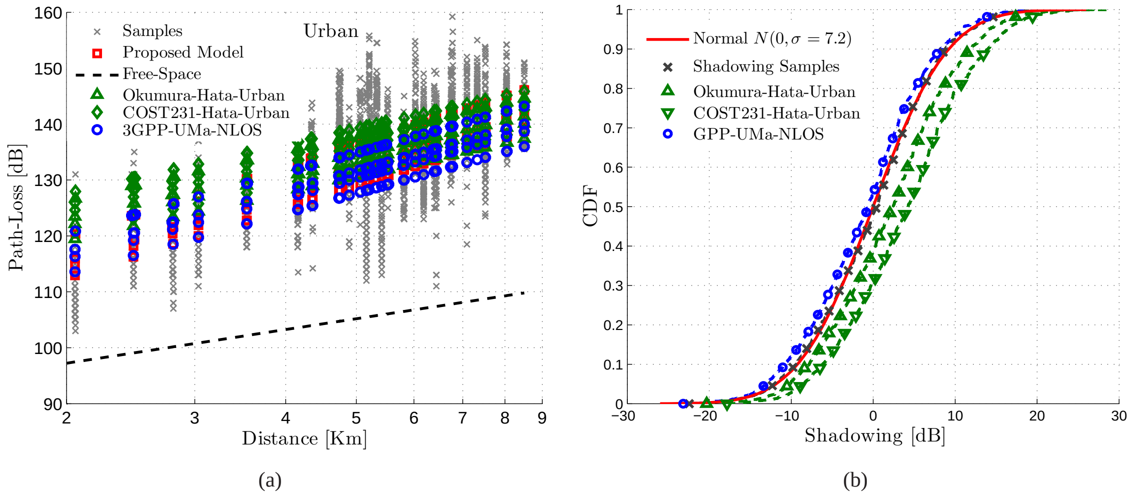

Fig. 11: Comparison of proposed PL model with other models in urban environment (a) and CDF of shadowing (b), Beirut city.

We also note the variability of NLOS conditions in this area that can be classified into moderately and heavily obstructed environments. In moderate NLOS conditions, small obstructions, such as trees or building edges partially block the direct path between ED and GW, whereas heavily obstructed NLOS conditions have large obstructions that fully block the direct path, leading to a higher PL. This high building shadow phenomenon may lead to non-covered areas in some locations. It should also be mentioned that the topography and the elevation profile influence the reception quality. For example, the presence of hills might block the reception as shown in Figure 10. It can be observed that LOS link is completely blocked in *Ras Beirut* located at 9 km from the GW, leading to no packet reception, while there is 90% PDR in *El Manara* located 8.5 m away due to the partially blocked LOS link.

The PL was modeled by log-distance model including the effect of ED antenna heights using equation (6). The fitting procedure has led to a PL exponent, a reference PL, an antenna loss factor equal to $n = 4.18$, $PL_0 = 102.86$, and $L_h = -6.3$, respectively. It is interesting to note the high value of n (larger than 2 in free-space conditions) due to the heavy density of the Beirut city (high density of buildings and obstructions). The shadowing samples in Figure 11b show a well-fitted Gaussian distribution with zero mean and $\sigma = 7.2$ dB. This error confirms the relevant impact of obstructions and reflections in the urban area. We have also compared the proposed model with the most used urban PL models namely Okumura-Hata for metropolitan areas, Cost 123-Hata and 3GPP-UMa as shown in Figure 11a. The free-space PL is plotted with a dashed black curve as a baseline model. The CDF of shadowing samples are also compared in Figure 11b. We can see that Okumura-Hata model and Cost 123-Hata predict higher PL values, which is also verified by the obtained mean of 2 dB, and 3.9 dB, respectively and an error standard deviation of 7.6 dB. More interestingly, 3GPP-UMa model shows relatively low predicted PL values with -1 dB as a mean error and 7.4 dB as a standard deviation. A good fit of the measured data is observed for distances lower than 5 km. This inaccuracy in the 3GPP-UMa model is due to the limitations of the base antenna height to 150 m as well as user antenna height to 1 m. However, the proposed model reduces the error and fits the samples with more accuracy compared to other models.

The effect of ED antenna height on LoRaWAN performance is also evaluated in Table VI. The results show that increasing ED antenna height improves the reliability of the link, *i.e.* increases the PDR and the SNR. From the results, we can see that PDR exceeds 0.85 even for a low antenna height (20 cm).

TABLE VI: Effect of h_{ED} on LoRaWAN Performance in urban environment.

h_{ED}	PDR	SNR	RSSI	min PDR	min SNR	min RSSI
20 cm	0.88	-3.52	-110.84	0.5	-11.76	-119.57
1.5 m	0.90	-0.28	-108.58	0.5	-10.56	-119.61
3 m	0.93	0.086	-107.31	0.7	-10.52	-118.16

It is worth to highlight here that an average PDR of 0.9 is achieved with a coverage area up to 9 km. One single GW is able to cover the majority of Beirut city. The location of the GW at 260 m above sea-level play a significant role in achieving this coverage. The absence of reception or the low PDR (0.5) in some locations is due to the presence of high construction density or to the topography area.

This article has been accepted for publication in a future issue of this journal, but has not been fully edited. Content may change prior to final publication. Citation information: DOI 10.1109/JIOT.2019.2906838, IEEE Internet of Things Journal

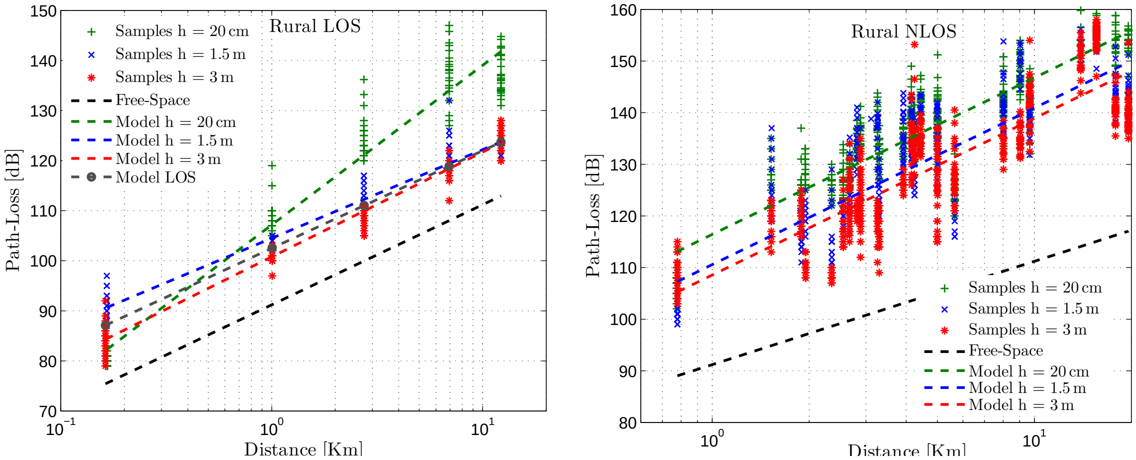

(a) (b)

Fig. 12: Path-loss model vs. distance in rural environment, (a) LOS, (b) NLOS, Bekaa valley.

An additional GW may be deployed to achieve higher performance and coverage. This shows the importance of carefully selecting the locations of the GWs to improve system reliability and capacity. We note that the lowest DR was used in our experiments, higher DR may be used in case of good communication links to reduce the transmission time and to increase the system throughput.

D. Outdoor Rural Results

In the rural environment, the radio path was identified as LOS link for an unobstructed path between the ED and GW antennas, and as NLOS link for the obstructed path. Similarly to the urban environment, various ED antenna heights were considered. Similar log-distance model in equation (6) is considered to derive the PL model.

Figure 12 illustrates the PL vs the distance for different ED antenna heights under LOS and NLOS conditions. The results show that the PL exponent is of 1.95 with ED antenna heights of 1.5 and 3 m, which is close to the free-space model. The standard deviation of shadowing is 2 to 3 dB. However, for h_{ED} = 20 cm, the LOS condition cannot be achieved due to the obstruction of the Fresnel zone by the ground as previously discussed. In the case of NLOS, similar behavior is observed compared to the urban case, where lowering the antenna height results in increasing the PL. We note that, in the case of rural environments, obstructions are mainly due to high vegetation, trees, mountains, etc. The presence of high density of vegetation can lead to a bad quality reception. The obtained PL exponent is $n = 3.033$, $PL_0 = 111.75$, and $L_h = -6.65$ dB. Compared to the urban area, the loss factor L_h is slightly higher. Hence, the impact of ED antenna height on improving the received signal is higher in the rural area due to fewer obstructions. The shadowing follows a Gaussian distribution with zero mean and $\sigma = 6.43$ dB (Figure 13b).

The proposed model was also compared to some exiting rural models namely Okumura-Hata model for open area and 3GPP-RMa model considering NLOS, as shown in Figure 13. In case of 3GPP-RMa model, two cases were considered. The first considers a street width W of 25 m, and the second has the maximum street width W of 50 m. We observed that Okumura-hata model underestimates the PL values and presents a mean and a standard deviation of -17 dB and 6.9 dB respectively. By adjusting the street width to 50 m, the 3GPP-Uma model is close to the samples with error mean and standard deviation of 1 dB and 6.9 dB, respectively. The proposed model shows lowest error of zero mean and standard deviation of 6.45 dB, thus indicating that the proposed model matches the measurements more accurately compared to other models. Next, the performance of LoRaWAN in terms of PDR and SNR was evaluated. Table VII summarizes the average and the minimum obtained values. These results validate those obtained in the urban scenario, where a similar impact of the antenna height on the reliability of LoRaWAN is observed. For instance, a minimum PDR of 0.25, 0.48 and 0.68 was observed with h_{ED} = 0.2, 1.5 and 3 m, respectively. This reliability can be improved by carefully adjusting the locations and the heights of both ED and GW. Control and retransmission, as well as ADR mechanisms, could also be used for further improvement. An average PDR above 0.9 is achieved, making LoRaWAN a promising technology for IoT applications in rural environments.

TABLE VII: LoRaWAN Performance in rural environment.

h_{ED}	PDR	SNR	RSSI	min PDR	min SNR	min RSSI
20 cm	0.90	-2.75	-107.71	0.24	-17.27	-118.7
1.5 m	0.92	2.08	-106.14	0.48	-14	-120
3 m	0.97	2.3	-102.57	0.68	-16	-118.4

Driving tests were also conducted in urban and rural environments (Figure 14). The results show that LoRaWAN EDs can communicate up to a distance of 9 km and 47 Km in urban and rural environments, respectively.

In general, we see from the results that LoRaWAN network with one GW gives satisfactory performance. The quality of reception and the communication range depends on different factors such as the density of obstructions (buildings, vegetation) as well as the terrain profiles in the outdoor area. In the indoor environment, the wall and floor penetration affect the transmission.

This article has been accepted for publication in a future issue of this journal, but has not been fully edited. Content may change prior to final publication. Citation information: DOI 10.1109/JIOT.2019.2906838, IEEE Internet of Things Journal

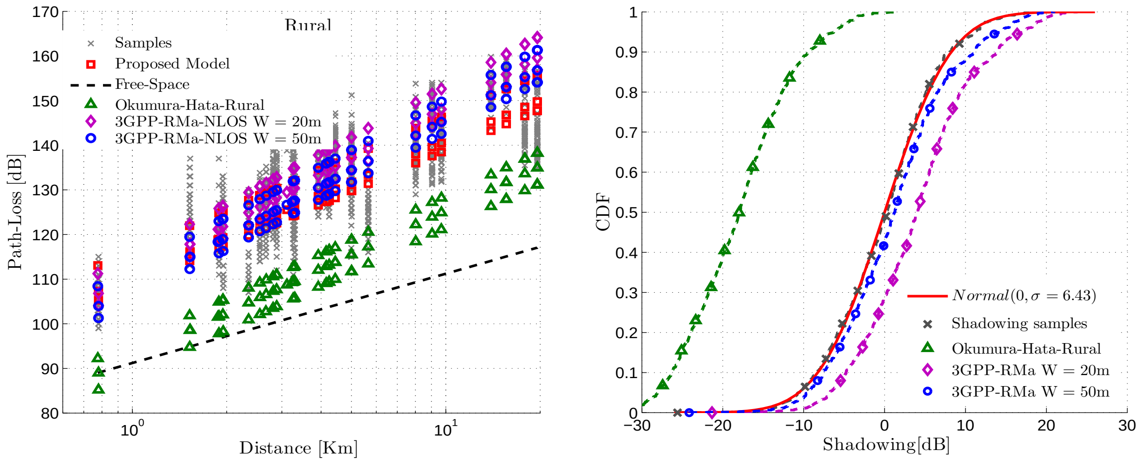

(a) (b)

Fig. 13: Comparison of proposed PL model with empirical models (a) and CDF of shadowing (b) in rural environment, Bekaa valley.

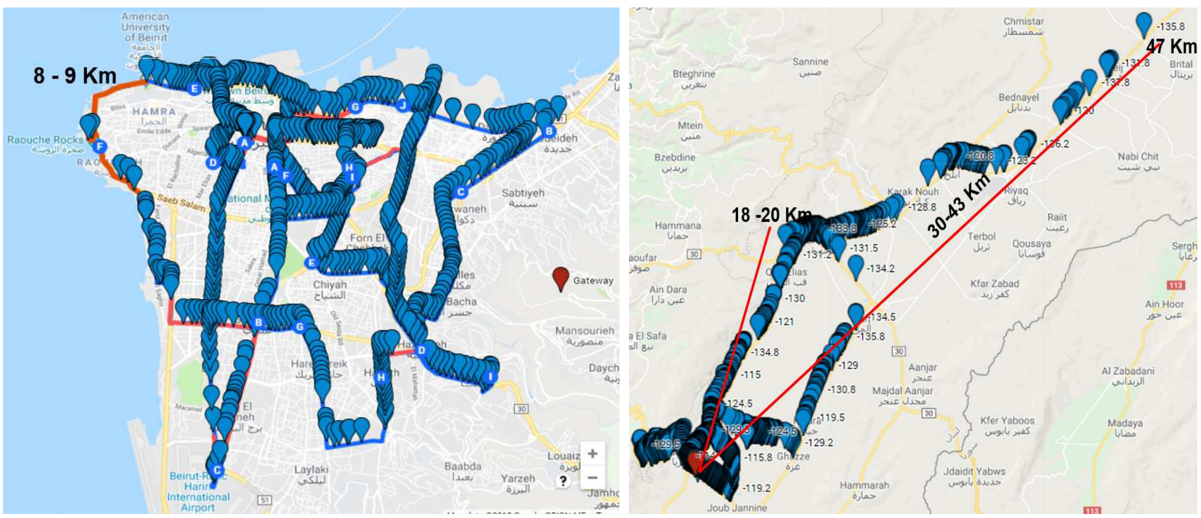

(a) Beirut City (b) Bekaa Valley

Fig. 14: Map of the drive test in urban (a) and (b) rural environment, coverage range up to 9 km (urban) and 47 m (rural).

A good selection of LoRaWAN GW locations achieves good coverage. The absence of reception in some locations, may be due to the presence of high construction density or elevation profile, which can be resolved by the installation of additional GWs. Table VIII summarizes the PL parameters and shadowing standard deviation for different tested environments. These proposed models are accurate and more simple to be used for estimating the communication range and for enabling more analysis of LoRaWAN performance in the areas similar to Lebanon.

TABLE VIII: Summary of PL characteristics and standard deviation of shadowing for various types of environments.

Metric	Indoor	Outdoor	Urban	Rural
PL exponent(n)	2.851	3.12	4.179	3.033
PL intercept(PL_0)	120.4	140.7	102.86	111.75
Shadow fading (σ)	8 dB	9.7 dB	7.2dB	6.4 dB
Wall/Floor Loss (L_w/L_f)	10/1.412	-	-	
ED height loss (L_h)	-	-4.7	-6.3	-6.65

VI. Conclusion

LoRaWAN has recently emerged as an attractive solution for low-power and long-range IoT communications. In this paper, an in-depth study of the radio propagation characteristics using LoRaWAN in several realistic environments under various ED antenna heights has been presented. The radio channel characterization is an essential issue in the design and deployment of communication systems. Therefore, extensive measurement campaigns were conducted in Lebanon in three different environments namely indoor, urban and rural. Indoor tests were carried-out in USJ campus. Urban tests were realized in Beirut city, whereas rural tests were realized in Bekaa valley. Based on the empirical measurements, PL models were further derived. Additionally, we compared the proposed models with several well used models. It was shown that the proposed models fit measurements with more accuracy and are much simple to be used in areas similar to Lebanon. Moreover, the performance of LoRaWAN was evaluated in terms of PDR and SNR. The reported results show the reliability of

LoRAWAN communications in real-life environments for long distances. In a dense urban area, a coverage range up to 9 km was attained, whereas in the rural case a coverage range up to 47 km was reached using a single deployed GW. The quality of transmission in high shadowing and blocking environments (buildings, elevation profile) can be improved by the installation of additional GWs and the optimization of GW locations. The performance results revealed the reliability of LoRaWAN for several IoT applications, such as smart cities, smart agriculture, etc. Future work can include other aspects such as adaptivity and scalability of LoRaWAN systems, network planning, and optimization of energy consumption.

Acknowledgment

This project has been jointly funded with the support of the National Council for Scientific Research in Lebanon CNRS-L and Saint Joseph University of Beirut.

References

[1] Cisco, "Embracing the Internet of Everything, Online: www.cisco.com," White paper, Tech. Rep., 2016.

[2] L. Atzori, A. Iera, and G. Morabito, "The Internet of Things: A survey," *Computer Networks*, vol. 54, no. 15, pp. 2787–2805, Oct. 2010.

[3] G. A. Akpakwu, B. J. Silva, G. P. Hancke, and A. M. Abu-Mahfouz, "A Survey on 5G Networks for the Internet of Things: Communication Technologies and Challenges," *IEEE Access*, vol. 6, pp. 3619–3647, 2018.

[4] U. Raza, P. Kulkarni, and M. Sooriyabandara, "Low Power Wide Area Networks: An Overview," *IEEE Communications Surveys Tutorials*, vol. 19, no. 2, pp. 855–873, Secondquarter 2017.

[5] J. de Carvalho Silva, J. J. P. C. Rodrigues, A. M. Alberti, P. Solic, and A. L. L. Aquino, "LoRaWAN - A low power WAN protocol for Internet of Things: A review and opportunities," in *2nd International Multidisciplinary Conference on Computer and Energy Science (SpliTech)*, July 2017, pp. 1–6.

[6] K. Mekkia, E. Bajica, F. Chaxela, and F. Meyerb, "A comparative study of LPWAN technologies for large-scale IoT deployment," *ICT express*, 2018.

[7] J. Finnegan and S. Brown, "A Comparative Survey of LPWA Networking," *ArXiv*, 2018.

[8] F. Adelantado, X. Vilajosana, P. Tuset-Peiro, B. Martinez, J. Melia-Segui, and T. Watteyne, "Understanding the Limits of LoRaWAN," *IEEE Communications Magazine*, 2017.

[9] K. Mikhaylov, J. Petaejaejaervi, and T. Haenninen, "Analysis of Capacity and Scalability of the LoRa Low Power Wide Area Network Technology," in *22th European Wireless Conference*, May 2016, pp. 1–6.

[10] M. C. Bor, U. Roedig, T. Voigt, and J. M. Alonso, "Do LoRa low-power wide-area networks scale?" in *19th ACM Int. Conf. Model. Anal. Simulat. Wireless Mobile Syst. (MSWiM)*, 2016, pp. 59–67.

[11] M. Stabicki, G. Premsankar, and M. D. Francesco, "Adaptive Configuration of LoRa Networks for Dense IoT Deployments," in *16th IEEE/IFIP Network Operations and Management Symposium (NOMS)*, Apr. 2018.

[12] U. Noreen, A. Bounceur, and L. Clavier, "A study of LoRa low power and wide area network technology," in *International Conference on Advanced Technologies for Signal and Image Processing (ATSIP)*, May 2017, pp. 1–6.

[13] A. Augustin, J. Yi, T. Clausen, and W. M. Townsley, "A Study of LoRa: Long Range & Low Power Networks for the Internet of Things," *Sensors*, 2016.

[14] O. Khutsoane, B. Isong, and A. M. Abu-Mahfouz, "IoT devices and applications based on LoRa/LoRaWAN," in 43^{rd} *Annual Conference of the IEEE Industrial Electronics Society (IECON)*, Oct 2017, pp. 6107–6112.

[15] J. M. Marais, R. Malekian, and A. M. Abu-Mahfouz, "LoRa and LoRaWAN testbeds: A review," in *IEEE AFRICON*, Sept 2017, pp. 1496–1501.

[16] P. Neumann, J. Montavont, and T. Noel, "Indoor deployment of low-power wide area networks (LPWAN): A LoRaWAN case study," in *IEEE 12th International Conference on Wireless and Mobile Computing, Networking and Communications (WiMob)*, Oct 2016, pp. 1–8.

[17] J. Petäjäjärvi, K. Mikhaylov, R. Yasmin, M. Hämäläinen, and J. Iinatti, "Evaluation of LoRa LPWAN Technology for Indoor Remote Health and Wellbeing Monitoring," *International Journal of Wireless Information Networks*, vol. 24, no. 2, pp. 153–165, Jun. 2017.

[18] L. Gregora, L. Vojtech, and M. Neruda, "Indoor signal propagation of LoRa technology," in *17th International Conference on Mechatronics - Mechatronika (ME)*, Dec 2016, pp. 1–4.

[19] K. E. Nolan, W. Guibene, and M. Y. Kelly, "An evaluation of low power wide area network technologies for the Internet of Things," in *International Wireless Communications and Mobile Computing Conference (IWCMC)*, Sept 2016, pp. 439–444.

[20] J. Petajajarvi, K. Mikhaylov, A. Roivainen, T. Hanninen, and M. Pettissalo, "On the coverage of LPWANs: range evaluation and channel attenuation model for LoRa technology," in *14th International Conference on ITS Telecommunications (ITST)*, Dec 2015, pp. 55–59.

[21] T. Petric, M. Goessens, L. Nuaymi, L. Toutain, and A. Pelov, "Measurements, performance and analysis of LoRa FABIAN, a real-world implementation of LPWAN," in *IEEE* 27^{th} *Annual International Symposium on Personal, Indoor, and Mobile Radio Communications (PIMRC)*, Sept 2016, pp. 1–7.

[22] S. Hosseinzadeh, M. Almoathen, H. Larijani, and K. Curtis, "A Neural Network Propagation Model for LoRaWAN and Critical Analysis with Real-World Measurements," *Big Data and Cognitive Computing*, 2017.

[23] R. Sanchez-Iborra, J. Sanchez-Gomez, J. Ballesta-Vinas, M.-D. Cano, and A. F. Skarmeta, "Performance Evaluation of LoRa Considering Scenario Conditions," *Sensors*, vol. 18, no. 3, p. 772, 2018.

[24] O. Iova, A. L. Murphy, G. P. Picco, L. Ghiro, D. Molteni, F. Ossi, and F. Cagnacci, "LoRa from the city to the mountains: Exploration of hardware and environmental factors," in *Int. Conf. Embedded Wireless Syst. Netw. (EWSN)*, 2017.

[25] G. del Campo, I. Gomez, S. Calatrava, R. Martinez, and A. Santamaria, "Power Distribution Monitoring Using LoRa: Coverage Analysis in Suburban Areas," in *International Conference on Embedded Wireless Systems and Networks (EWSN)*, 2018.

[26] P. Ferrari, A. Flammini, S. Rinaldi, M. Rizzi, and E. Sisinni, "On the use of LPWAN for EVehicle to grid communication," in *AEIT International Annual Conference*, Sept 2017, pp. 1–6.

[27] N. Hayati and M. Suryanegara, "The IoT LoRa system design for tracking and monitoring patient with mental disorder," in *IEEE International Conference on Communication, Networks and Satellite (Comnetsat)*, Oct 2017, pp. 135–139.

[28] A. Mdhaffar, T. Chaari, K. Larbi, M. Jmaiel, and B. Freisleben, "IoT-based health monitoring via LoRaWAN," in *IEEE EUROCON* 17^{th} *International Conference on Smart Technologies*, July 2017, pp. 519–524.

[29] W. Guibene, J. Nowack, N. Chalikias, K. Fitzgibbon, M. Kelly, and D. Prendergast, "Evaluation of LPWAN Technologies for Smart Cities: River Monitoring Use-Case," in *IEEE Wireless Communications and Networking Conference Workshops (WCNCW)*, March 2017, pp. 1–5.

[30] Y. Okumura, E. O. andT. Kawano, and K. Fukuda, "Field strength and its variability in VHF and UHF land mobile radio service," *Review of the Electrical Communications Laboratories*, 1968.

[31] E. . COST Action 231, European Communities, "Digital mobile radio towards future generation systems, final report," , Tech. Rep., 1999.

[32] I.-R. M.2135-1, "Guidelines for evaluation of radio interface technologies for IMT-Advanced," , Tech. Rep., 2009.

[33] W. II, "Winner II channel models: Deliverable 1.1.2," , Tech. Rep., 2008.

[34] , "D5.3: WINNER+ Final Channel Models," CELTIC, Tech. Rep., 2010.

[35] ——, "Further advancements for E-UTRA physical layer aspects," 3GPP TR 36.814 v9.0.0, Tech. Rep., 2010.

[36] ——, "Propagation data and prediction methods for the planning of indoor radio communication systems and the radio local area networks in the frequency range 900 MHz to 100 GHz," ITU-R Recommendations, Tech. Rep., 2001.

[37] V. Erceg, L. Schumacher, and P. Kyritsi, "Tgn channel models : IEEE P802.11Wireless LANs," , Tech. Rep., 2004.

[38] M. Lott and I. Forkel, "A Multi-Wall-and-Floor Model for Indoor Radio Propagation," in *IEEE Vehicular Technology Conference (VTC)*, May 2011, pp. 64 – 468.

[39] P. Jörke, S. Böcker, F. Liedmann, and C. Wietfeld, "Urban channel models for smart city IoT-networks based on empirical measurements of LoRa-links at 433 and 868 MHz," in *2017 IEEE 28th Annual International Symposium on Personal, Indoor, and Mobile Radio Communications (PIMRC)*, Oct 2017, pp. 1–6.

[40] S. Hosseinzadeh, H. Larijani, K. Curtis, A. Wixted, and A. Amini, "Empirical propagation performance evaluation of lora for indoor en-

vironment," in *2017 IEEE 15th International Conference on Industrial Informatics (INDIN)*, July 2017, pp. 26–31.
[41] LoRaWAN Measurement Campaigns in Lebanon. [Online]. Available: https://zenodo.org/record/1560654
[42] Semtech, "LoRa Modem Design Guide, rev.1," Semtech, Tech. Rep., Jul. 2013.
[43] B. Reynders and S. Pollin, "Chirp spread spectrum as a modulation technique for long range communication," in *Symposium on Communications and Vehicular Technologies (SCVT)*, Nov 2016, pp. 1–5.
[44] N. Sornin, M. Luis, T. Eirich, T. Kramp, and O. Hersent, "LoRaWAN specification version 1.0 ," LoRa Alliance, Tech. Rep., Jan. 2015.
[45] E. E. . 220-2, "Short Range Devices (SRD) operating in the frequency range 25 MHz to 1 000 MHz; Part 2: Harmonised Standard covering the essential requirements of article 3.2 of Directive 2014/53/EU for non specific radio equipment ," , Tech. Rep., 2017.
[46] [Online]. Available: https://docs.pycom.io/
[47] [Online]. Available: https://www.kerlink.com/product/wirnet-station/

Rida El Chall received the B.E degree in telecommunications and computer engineering from the faculty of engineering at Lebanese university, Lebanon, in 2012, and the M.S degree in Micro-technologies, architecture, networks and communication systems in 2012, and the Ph.D. degree in telecommunication and electronic engineering from the Institut National des Sciences Appliquées (INSA), Rennes, France, in 2015. From 2016 to 2017, she worked as a Research Engineer at CEA-Leti, France. She joined ESIB-USJ as a Research Assistant for 6 months, working on wireless communication for the internet of things. Her research interests lie in the area of digital communications, wireless networking and Internet of Things.

Samer Lahoud is an Associate Professor at the Saint-Joseph University of Beirut where he lectures computer networking courses at the Faculty of engineering (ESIB). His research activities focus on routing and resource allocation algorithms for wired and wireless communication networks. He has co-authored more than 80 papers published in international journals and conference proceedings. Mr. Lahoud received the Ph.D. degree in communication networks from Telecom Bretagne, Rennes, in 2006. After his Ph.D. degree, he spent one year at Alcatel-Lucent Bell Labs Europe. From 2007 to 2016, he was with the University of Rennes 1 and with IRISA Labs Rennes as an Associate Professor.

Melhem El Helou (S'08–M'15–SM'19) received the engineer's degree and master's degree in telecommunications and networking engineering from the Ecole Supérieure d'Ingénieurs de Beyrouth (ESIB), Faculty of Engineering at the Saint Joseph University of Beirut, Beirut, Lebanon, in 2009 and 2010, respectively and the Ph.D. degree in computer and telecommunications engineering from IRISA Research Institute, University of Rennes 1, Rennes, France and Saint Joseph University of Beirut, in 2014. He joined ESIB in September 2013 where he is currently an Assistant Professor (fr: Maître de conférences). His research interests include wireless networking, Internet of things, and quality of service.